Two-photon-resonant four-wave-mixing spectroscopy of atomic hydrogen in flames

Jeffrey A. Gray [1] and Rick Trebino

Combustion Research Facility, Sandia National Laboratories, Livermore, CA 94551-0969, USA

Received 20 July 1993; in final form 8 October 1993

We report a new diagnostic technique based on resonant four-wave-mixing spectroscopy of the two-photon 1s→2s transition in atomic hydrogen. Observations including Doppler-free spectral lineshapes and saturation behavior are related to models for the nonlinear optical processes. Two-photon wave-mixing measurements of atomic hydrogen concentration in laboratory flames at pressures of 30–760 Torr appear to be less susceptible to errors from collisional quenching than similar measurements made using laser-induced fluorescence.

1. Introduction

Atomic hydrogen (H) is an important free-radical species in the chemistry of flames and plasmas, and measurements of H concentration ([H]) are valuable tests of chemical kinetic models [1,2]. The accuracy of existing optical probes for [H] has rarely been sufficient to allow meaningful comparisons with such models, primarily because of uncertainties in accounting for the collisional environment. Here we describe a new coherent spectroscopic method based on two-photon-resonant four-wave-mixing for monitoring [H] in laboratory flames. We also present spectra, laser intensity dependencies, and relative [H] measurements that support our theoretical description of the nonlinear optical processes.

A variety of multiphoton excitation techniques have been developed for detecting H in environments such as flames that are opaque at its vacuum-ultraviolet resonance absorption wavelengths. Several different schemes based on detecting laser-induced fluorescence (LIF) have been reported [3–8]. While LIF offers very high detection sensitivity, species-dependent collisional quenching can introduce significant errors. Multiphoton ionization techniques have also been used with some success [9–12].

Alternatively, methods that generate a coherent signal beam have inherent advantages when optical access is limited or when background luminosity is present at the detection wavelength. Examples of such methods include stimulated emission (SE) [13,14], polarization spectroscopy (PS) [15], third harmonic generation (THG) [16], and laser-induced grating spectroscopy (LIGS) [17]. Unfortunately, SE signals are difficult to quantify, THG operates in the vacuum ultraviolet, and PS is relatively insensitive. While LIGS provides a quantifiable, coherent signal beam at convenient wavelengths, it suffers quenching problems very similar to those in LIF-based measurements.

Two-photon four-wave-mixing (2P4WM) spectroscopy has been applied previously in the gas phase to only a few stable species [18–20]. Here we show that 2P4WM is a sensitive diagnostic for free radicals and that 2P4WM can be more quantitative than incoherent methods because it depends on the total dephasing rate of a transition rather than on specific population relaxation processes such as collisional quenching. The optical process in 2P4WM is quite similar to that in coherent anti-Stokes Raman spectroscopy (CARS) [#1] and resonant sum-frequency generation.

[1] New address: Department of Chemistry, Ohio Northern University, Ada, OH 45810, USA.

SSDI 00009-2614(93)E1288-R

2. Experimental

We used a Q-switched Nd:YAG-pumped dye laser operating near 486 nm to generate 2P4WM and LIF signals in this study. The dye laser output was frequency doubled in β-barium borate to produce 7 ns pulses having a bandwidth of $\Delta\nu = 0.4$ cm^{-1} and energies up to 1.5 mJ at 243 nm. Fig. 1 shows a schematic of the experiment including optical elements and laser beams paths. We first passed the 243 nm beam trough a variable attenuator and then split it into three beams of roughly equal intensity.

Two of these beams, labeled "f" and "b" for forward and backward pump, respectively, were focused with 750 mm lenses and crossed at an angle of 178° (nearly counter-propagating) to overlap above the surface of a flat-flame burner. We carefully reduced the difference in optical paths for these two beams to a fraction of their pulse coherence length ($l_c = (2\ln 2/\pi)^{0.5}/\Delta\nu \approx 1.6$ cm) to optimize their interaction in the sample region. The third beam, labeled "p" for probe, was focused and crossed at an angle of 2° with the "f" beam in the overlap region (diameter ≈ 0.15 mm, length ≈ 30 mm). The "p" beam path included a retroreflector to adjust the arrival time of that pulse between ±170 ps (±5 cm) relative to the "f" and "b" pulses. Vector phase matching was achieved for these three beams as shown in the inset of fig. 1.

We used a thin quartz cuvette (1 mm) and a 0.1 mM solution of DCM dye in methanol to optimize the spatial and temporal overlap of the input beams and generate a signal alignment beam to direct through an aperture, a 200 mm f.l. lens, and a 50 μm pinhole. This spatial filter greatly reduced the amount of scattered 243 nm light passing through a 240–10 nm bandpass filter to a photomultiplier (PMT).

We attenuated the 486 nm fundamental beam from the dye laser, reduced it to a diameter of ≈ 1 mm, and overlapped it with the 243 nm beams in the sample region. We monitored the pulse energies in the 243 and 486 nm beams using photodiodes and sampled LIF at the side of the flame through a 486 nm bandpass filter using a PMT. Finally, we recorded the outputs from all of the detectors by integrating, digitizing, and averaging typically 40 laser pulses.

3. Theory

Fig. 2 shows the energy levels of atomic hydrogen labeled according to principle quantum number n. Multi-photon transitions connect the $n = 1$, 2, and 4 levels at laser frequencies $\omega_{ex} = 243$ nm and $\omega_{pr} = 486$ nm. Diagram (a) illustrates the basic 2P4WM process. Using nonlinear-optical perturbation theory [21], we derive the peak signal for this process,

[#1] Excluding electronic resonance-enhanced CARS schemes.

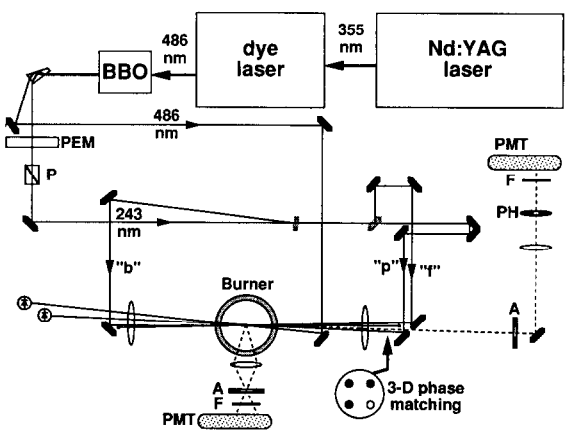

Fig. 1. Schematic of the optical path in two-photon four-wave-mixing experiments. Elements are labeled as PEM for photoelestic modulator, P for polarizer, A for iris aperture, PH for pinhole, F for filter, and PMT for photomultiplier tube.

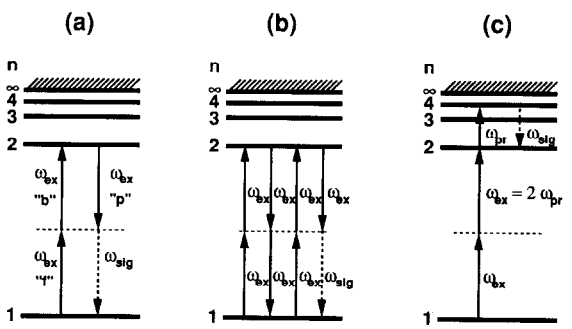

Fig. 2. Energy levels for atomic hydrogen labeled according to principle quantum number n. Transition frequencies involved in (a) two-photon four-wave mixing, (b) two-photon eight-wave mixing, and (c) two-color laser-induced fluorescence.

$$S_{2P4WM} \propto |\chi^{(3)}|^2$$
$$\propto [H]^2(\alpha_{12})^2 I_f I_b I_p L^2 |g(\delta_{ex}, \Gamma_{12})|^2 , \quad (1)$$

where $\chi^{(3)}$ is the third-order nonlinear susceptibility; [H] is the atomic hydrogen concentration; α_{12} is the peak two-photon cross section of the 1s→2s transition; I_i are the intensities of the input beams; L is the overlap path length; and $g(\delta, \Gamma) \equiv i/(1+i\delta/\Gamma)$ is a Lorentzian line shape function in terms of the detuning $\delta_{ex}=\omega_{12}-(\omega_f+\omega_b)$ and the dephasing rate Γ_{12}. The frequency and wave vector of the signal beam are given by

$$\omega_{sig}=\omega_f+\omega_b-\omega_p , \quad (2a)$$
$$k_{sig}=k_f+k_b-k_p . \quad (2b)$$

Other four-wave-mixing processes (i.e. different time orderings) are nonresonant and hence negligible or do not contribute because of phase-matching constraints.

The 2P4WM process diagrammed in fig. 2a is properly described as a coherence phenomenon. Unlike one-photon-resonant degenerate four-wave-mixing (DFWM) or the two-photon eight-wave-mixing (2P8WM) process shown in fig. 2b that involve population gratings, 2P4WM involves a coherence that oscillates in time at $2\omega_{ex}$ but is uniform in space. In addition, 2P4WM is independent of gas velocity (i.e. Doppler free) in the geometry shown in fig. 1 [22]. Doppler-free 2P4WM thus probes all atoms rather than just those having a particular velocity, resulting in a greatly improved sensitivity. Spectrally integrated 2P4WM signals vary as the dephasing time $(1/\Gamma_{12})$ but are not directly affected by the population relaxation time.

2P8WM (fig. 2b) is a higher-order process that can occur simultaneously with 2P4WM at the same frequency and wave vector. 2P8WM is the two-photon analog of resonant DFWM and does involve lifetime effects such as population gratings. The signal in 2P8WM, however, is proportional to $|\chi^{(7)}|^2$ and I_{ex} [7] and hence is not expected to be important except at very high intensities.

We compare the results of 2P4WM experiments with those from a two-color LIF process involving two-photon absorption to the 2s level followed by resonant fluorescent excitation to the 4p state (fig. 2c). Both LIF resonances are conveniently achieved using the same dye laser since $\omega_{12} \approx 4\omega_{24}$ in atomic hydrogen [7]. The peak LIF signal is [17]

$$S_{LIF} \propto \mathrm{IM}(\chi^{(5)}) \propto [H]\alpha_{12}\sigma_{24}\tau_2\tau_4 I_{ex}^2 I_{pr} L A_{42}$$
$$\times \mathrm{Im}[g(\delta_{ex}, \Gamma_{12})]\,\mathrm{Im}[g(\delta_{pr}, \Gamma_{24})] , \quad (3)$$

where τ_2 and τ_4 are lifetimes of the 2s and 4p states, A_{42} is the spontaneous emission rate, and the excitation and probe steps are considered incoherent. Compared to 2P4WM, the LIF signal has lower-order dependencies on α_{12} and I_{ex} but is has a direct dependency on the lifetimes τ_2 and τ_4. Eqs. (1) and (3) do not contain saturation effects.

4. Results

Fig. 3 shows a 2P4WM spectrum of atomic hydrogen recorded 10 mm above the burner surface in a slightly rich ($\phi=1.2$) 92 Torr $H_2/O_2/N_2$ flame (N_2 mole fraction = 0.26) using total pulse energies of 300 μJ at 243 nm. The laser bandwidth mainly limits the observed spectral line width, although the asymmetry in the lineshape suggests that optical Stark broadening is also occurring. The Doppler-broadened width of the LIF signal under these conditions is approximately twice that of 2P4WM. The width of the 2P4WM line increases slightly in these flames at pressures between 90 and 760 Torr as the homogenous transition width Γ_{12} becomes comparable to that of the multimode laser.

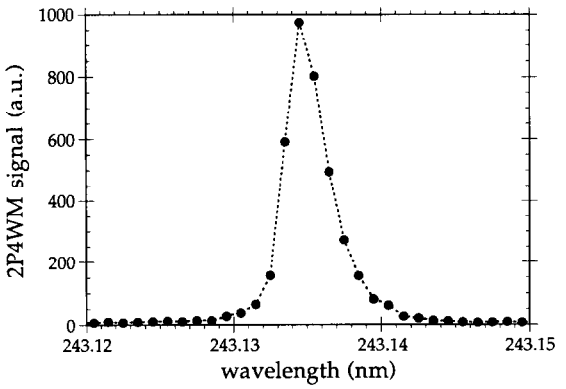

Fig. 3. Two-photon four-wave-mixing (2P4WM) spectrum of atomic hydrogen in a 92 Torr $H_2/O_2/N_2$ flame. The observed line width (0.5 cm^{-1}) is slightly larger than the probe laser bandwidth (0.4 cm^{-1}) for laser pulse intensities of 0.3 GW/cm^2.

The peak intensity of the 2P4WM signal decreases with increasing pressure as expected from relation (1), in which $\alpha_{12} \propto 1/\Gamma_{12}$, although the changes in flame structure over this pressure range make it difficult to compare relative signal intensities. The nonzero baseline signal in fig. 3 is due to scattered 243 nm light. We also observe a non-resonant wave-mixing background signal at pressures above 90 Torr, especially in hydrocarbon flames.

The variable attenuator shown in fig. 1 preserves the alignment and spatial properties of the input beams. The data points in fig. 4 show the observed 2P4WM and LIF signals from H atoms in a 30 Torr flame as a function of total input pulse energy at 243 nm. At energies below 300 μJ (0.25 GW/cm^2), the signals increase as I^n, where $n=2$ for LIF and $n=3$ for 2P4WM. At higher energies, a simple incoherent rate model for the LIF, including two-photon coupling at ω_{12} and one-photon ionization from $n=2$, predicts saturation of the form

$$\text{signal} \propto \frac{I_{ex}^n}{1 + W_i \tau_2 I_{ex} + (I_{ex}/I_{sat})^2}. \quad (4)$$

Using estimates of $W_i = 5$ cm^2/W ns for the ionization rate coefficient [4] and $\tau_2 = 0.6$ ns for a 30 Torr flame [23], least-squares fitting of the data in fig. 4 yields the solid curve with $I_{sat} \approx 450$ μJ for LIF. Eq. (4) also provides an empirical fit to the 2P4WM saturation behavior with $I_{sat} \approx 300$ μJ. At 760 Torr the 2P4WM shows no signs of saturation at energies up to 600 μJ.

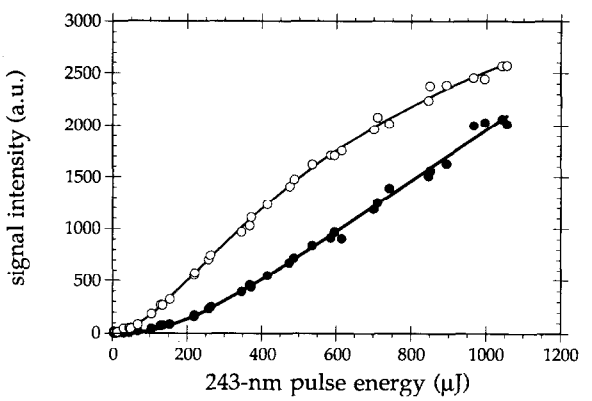

Fig. 4. Measured (●) two-photon four-wave-mixing (2P4WM) and (○) LIF signals as a function of 243 nm pulse energy (symbols), and modeled saturation behavior (curves) in a 30 Torr flame.

The 486 nm beam has no effect on the 2P4WM signal at low pulse energies (< 5 μJ) but causes saturation of the LIF signal because of the large oscillator strength of the 2s↔4p transition. However, above 20 μJ the 486 nm beam causes a noticeable decrease in the 2P4WM signal, which reaches ≈ 1/3 of its original value for 486 nm pulse energies of 1 mJ. This reduction in 2P4WM signal probably results from power broadening of the 2s↔4p transition, which causes additional dephasing of the 2s state beyond that due to collisions. Of course, 2P4WM is not normally to be performed with the 486 nm beam present.

We obtain an upper limit for the dephasing time in 2P4WM by delaying the "p" pulse. The observed "coherence spike" arises from picosecond structure within the 7 ns laser pulses and can provide information similar to that from ultrafast experiments [24]. The observed fwhm of the 2P4WM coherence peak for H in our 30 Torr flames is the same as that we observe using a liquid solution of DCM in methanol where we expect dephasing to be very fast, suggesting that in both cases the fwhm is limited by the laser's coherence time (50 ps).

We measured [H] as a function of height above the burner surface by translating the burner. Fig. 5 shows a comparison of [H] profiles measured in a slightly rich ($\phi = 1.2$) 30 Torr $H_2/O_2/N_2$ flame using 2P4WM and LIF signals and the [H] and I_{ex} dependencies from relations (1) and (3). The solid

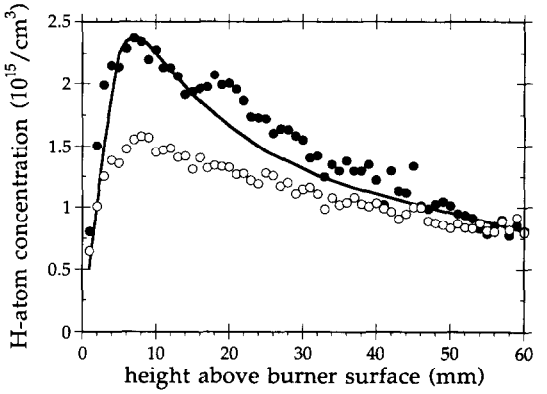

Fig. 5. Atomic hydrogen concentration in a 32 Torr $H_2/O_2/N_2$ flame. The experimental traces are scaled to match the calculation at $x = 60$ mm. LIF signals are systematically smaller near the burner surface because of the larger collisional quenching rate in this region. (●) 2P4WM, (○) LIF, (——) chemistry model.

curve is the [H] profile predicted using a chemical kinetic model for this flame [25,26]. The measured profiles are scaled to match the model in the post-flame region at $x=60$ mm. Our [H] measurements derived from 2P4WM are consistently larger and in better agreement with the model results than those from LIF in the flame region ($x \approx 10$ mm at 30 Torr); however, the 2P4WM measurements are noisier than LIF because of larger pulse-to-pulse fluctuations. These observations are insensitive to experimental conditions such as the laser pulse energy in the 243 or 486 nm beams.

5. Discussion

The fundamental difference between 2P4WM and multi-photon LIF is in their scaling with [H] and τ. The $[H]^2$ dependency of 2P4WM is a distinct disadvantage at low concentrations, especially when the detection sensitivity is limited by non-resonant background or scattered light. However, since [H] often exceeds 10^{14} atoms/cm^3 in many flame or plasma environments, the sensitivity of 2P4WM should not be a problem. Furthermore, a detection limit of less than 10^{13} H atoms/cm^3 should be possible using narrow-bandwidth lasers when the homogeneous line width is ≈ 0.04 cm^{-1} (e.g. a 30 Torr flame). The non-resonant background problem in 2P4WM appears to be difficult to avoid, as in CARS, and the good signal-to-background ratio for 2P4WM at H mole fractions of $\approx 1\%$ is due mainly to a favorable two-photon absorption cross section.

The dependency of 2P4WM signals on dephasing rather than directly on lifetime should enable improved accuracy of [H] measurements, especially when the lifetime varies strongly within the measurement region. Collisional quenching rates for H are difficult to measure because they exceed radiative decay rates in many combustion or plasma conditions. Quenching is also difficult to model because it depends on local species concentration and temperature [23,27–29]. Quenching rates in low-pressure $H_2/O_2/N_2$ flames peak in the pre-flame gases [23,29], causing LIF measurements to under-represent [H] near the burner surface. This effect is seen clearly in fig. 5.

Alternatively, dephasing, which is expected to be proportional to total collider density, does not vary strongly in low-pressure flames and has been measured to be $\approx 10\times$ faster than quenching [30]. In any case, high-resolution measurements of the line width could be used to account directly for variations in dephasing that affect 2P4WM signals. Alternatively, 2P4WM could be performed with a fixed dephasing rate by using the 486 nm beam, at photochemically insignificant intensities, to control the line width in a manner analogous to the LIF-based technique of photoionization-controlled loss spectroscopy [4,29,31].

Although eq. (1) predicts that 2P4WM signals should increase rapidly with laser pulse energy, several effects restrict the utility of such an approach. As seen in fig. 4, saturation of the resonant signal occurs for energies greater than 300 μJ while the non-resonant background continues to increase as I^3. The increased importance of 2P8WM and 2+1 resonant multi-photon ionization also degrade the accuracy of 2P4WM at higher intensity. Finally, LIF studies have shown that photochemical production of H by 243 nm probe beams is a problem at intensities > 1 GW/cm^2 in $H_2/O_2/N_2$ flames [32].

In conclusion, 2P4WM spectroscopy, as described here for atomic hydrogen, should be applicable to other atoms or molecules having suitable two-photon absorption strengths. Atomic oxygen (O), nitrogen (N), carbon (C), fluorine (F) and chlorine (Cl) have strong two-photon transitions at wavelengths [33] that are convenient for 2P4WM. Therefore, a coherent detection scheme such as 2P4WM for these species should overcome collision-induced uncertainties in LIF-based concentration measurements.

Acknowledgement

The authors would like to thank Dr. D.W. Chandler and Dr. L.A. Rahn for many valuable insights. This work was supported by the US Department of Energy, Office of Basic Energy Sciences, Chemical Sciences Division.

References

[1] J.E.M. Goldsmith, J.A. Miller, R.J.M. Anderson and L.R. Williams, Twenty-third Symposium (International) on Combustion (1990) 1821.

[2] J.A. Miller, J.V. Volponi, J.L. Durant Jr., J.E.M. Goldsmith, G.A. Fist and R.J. Kee, Twenty-third Symposium (International on Combustion (1990) 187.

[3] J.E.M. Goldsmith, Opt. Letters 10 (1985) 116.

[4] J.T. Salmon and N.M. Laurendeau, Appl. Opt. 26 (1987) 2881.

[5] J.E.M. Goldsmith, Twenty-second Symposium (International) on Combustion (1988) 1403.

[6] J. Bittner, K. Kohse-Hoinghaus, U. Meier, S. Kelm and T. Just, Combustion Flame 71 (1988) 41.

[7] J.E.M. Goldsmith and N.M. Laurendeau, Opt. Letters 15 (1990) 576.

[8] A.D. Tserepi, J.R. Dunlop, B.L. Preppernau and T.A. Miller, J. Appl. Phys. 72 (1992) 2638.

[9] G.C. Bjorkman, C.P. Ausschnitt, R.R. Freeman and R.H. Storz, Appl. Phys. Letters 33 (1978) 54.

[10] J.E.M. Goldsmith, Opt. Letters 7 (1982) 437.

[11] J.E.M. Goldsmith, Twentieth Symposium (International) on Combustion (1984) 1331.

[12] K.C. Smyth and P.J.H. Tjossem, Appl. Opt. 29 (1990) 4891.

[13] J.E.M. Goldsmith, J. Opt. Soc. Am. B 6 (1989) 1979.

[14] R.C.Y. Auyeung, D.G. Cooper, S. Kim and B.J. Feldman, Opt. Commun. 79 (1990) 207.

[15] K. Danzmann, K. Grutzmacher and B. Wende, Phys. Rev. Letters 57 (1986) 2151.

[16] F.G. Celii, H.R. Thorsheim, J.E. Butler, L.S. Plano and J.M. Pinneo, J. Appl. Phys. 68 (1990) 3814.

[17] J.A. Gray, J.E.M. Goldsmith and R. Trebino, Opt. Letters 18 (1993) 444.

[18] D.G. Steel and J.F. Lam, Phys. Rev. Letters 43 (1979) 1588.

[19] G. Meyer and D.W. Chandler, Chem. Phys. Letters 192 (1992) 1.

[20] N. Georgiev, U. Westblom and M. Alden, Opt. Commun. 94 (1992) 99.

[21] Y. Prior, IEEE J. Quantum Electron. QE-20 (1984) 37.

[22] T.-Y. Fu and M. Sargent III, Opt. Letters 5 (1980) 433.

[23] J.E.M. Goldsmith, R.J.M. Anderson and L.R. Williams, Opt. Letters 15 (1990) 78.

[24] N. Morita, T. Tokizaki and T. Yajima, J. Opt. Soc. Am. B 4 (1987) 1269.

[25] R.J. Kee, J.F. Grcar, D.M. Smooke and J.A. Miller, A Fortran program for modeling steady laminar one-dimensional premixed flames, report SAND85-8240, Sandia National Laboratories (1985).

[26] R.J. Kee, J.A. Miller and T.J. Jefferson, CHEMKIN: A general-purpose, problem-independent, transportable, Fortran chemical kinetics code package, report SAND80-8003, Sandia National Laboratories (1980).

[27] U. Meier, K. Kohse-Hoinghaus and T. Just, Chem. Phys. Letters 126 (1986) 567.

[28] J. Bittner, K. Kohse-Hoighaus, U. Meier and T. Just, Chem. Phys. Letters 143 (1988) 571.

[29] J.T. Salmon and N.M. Laurendeau, J. Quant. Spectry. Radiative Transfer 43 (1990) 155.

[30] J.E.M. Goldsmith and L.A. Rahn, Opt. Letters 15 (1990) 814.

[31] R.P. Lucht, J.T. Salmon, G.B. King, D.W. Sweeney and N.M. Laurendeau, Opt. Letters 8 (1983) 365.

[32] J.E.M. Goldsmith, Appl. Opt. 28 (1989) 1206.

[33] W.K. Bischel, B.E. Perry and D.R. Crosley, Appl. Opt. 21 (1982) 1419.